JACS
JOURNAL OF THE AMERICAN CHEMICAL SOCIETY

ARTICLE

pubs.acs.org/JACS

Selective Homogeneous Hydrogenation of Biogenic Carboxylic Acids with [Ru(TriPhos)H]$^+$: A Mechanistic Study

Frank M. A. Geilen,[†] Barthel Engendahl,[†] Markus Hölscher,[†] Jürgen Klankermayer,*[,†] and Walter Leitner*[,†,‡]

[†]Institut für Technische und Makromolekulare Chemie, RWTH Aachen University, Worringerweg 1, 52074 Aachen, Germany

[‡]Max-Planck-Institut für Kohlenforschung, Kaiser-Wilhelm-Platz 1, 45470 Mülheim a.d. Ruhr, Germany

Supporting Information

ABSTRACT: Selective hydrogenation of biogenic carboxylic acids is an important transformation for biorefinery concepts based on platform chemicals. We herein report a mechanistic study on the homogeneously ruthenium/phosphine catalyzed transformations of levulinic acid (LA) and itaconic acid (IA) to the corresponding lactones, diols, and cyclic ethers. A density functional theory (DFT) study was performed and corroborated with experimental data from catalytic processes and NMR investigations. For [Ru(TriPhos)H]$^+$ as the catalytically active unit, a common mechanistic pathway for the reduction of the C═O functionality in aldehydes, ketones, lactones, and even free carboxylic acids could be identified. Hydride transfer from the Ru−H group to the carbonyl or carboxyl carbon is followed by protonation of the resulting Ru−O unit via σ-bond metathesis from a coordinated dihydrogen molecule. The energetic spans for the reduction of the different functional groups increase in the order aldehyde < ketone < lactone ≈ carboxylic acid. This reactivity pattern as well as the absolute values are in full agreement with experimentally observed activities and selectivities, forming a rational basis for further catalyst development.

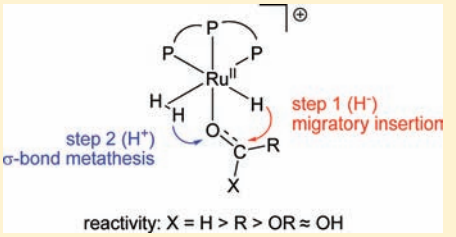

INTRODUCTION

The selective catalytic conversion of biomass feedstock is an important challenge for synthetic chemistry to build novel sustainable supply chains for the production of transportation fuels and industrial chemicals.[1,2] Lignocellulose constitutes a major fraction of the terrestrial biomass feedstock, and therefore much scientific and industrial attention is paid on its conversion to valuable products.[3,4] A widely studied approach is the conversion of the carbohydrate fraction of lignocellulose into a set of defined platform molecules, which are used as key intermediates for the synthesis of novel fuels and fuel additives.[5,6] The implementation of the concept of platform chemicals requires a detailed understanding of the molecular principles regulating their further transformations resulting in multistep reaction cascades and synthetic networks.

A general theme in the synthetic pathways from carbohydrate feedstocks is the reduction of the oxygen content via hydrogenation and dehydration sequences. This is illustrated in Scheme 1 for the two potential platform chemicals levulinic acid (LA) and itaconic acid (IA) yielding a set of isomeric lactones, diols, and cyclic ethers. Recently, we have developed a catalytic system consisting of a ruthenium precursor such as Ru(acac)$_3$ (**1**), the ligand TriPhos (TriPhos = 1,1,1-tris(diphenylphosphinomethyl)ethan, **2**), and an acidic additive (Chart 1), which allows the selective synthesis of each of the individual products in over 90% yield.[7] In the present paper, we describe a combined experimental and theoretical study on a plausible molecular mechanism of this system, which allows rationalizing the observed reactivities and selectivities toward the different functional groups in this reaction network.

Ruthenium/phosphine complexes have found application as hydrogenation catalysts and especially complexes with the facially coordinating tridentate ligand TriPhos have been identified to form highly active catalysts for the hydrogenation of esters, amides, and even free carboxylic acids.[7−16] Bianchini and co-workers reported on the reactivity of Ru/TriPhos complexes toward various substrates in hydrogenation reactions,[17−19] and studied its complexes extensively by NMR and IR spectroscopy.[20] They were able to characterize Ru/TriPhos complexes containing a dihydrogen molecule as ligand in solution by low-temperature and/or high-pressure NMR techniques.[21−23] The presence of a nonclassical hydrogen molecule also could be proved for Ir/TriPhos and Rh/Triphos complexes. Cationic dihydrogen complexes of ruthenium were shown to be active hydrogenation catalysts also with mono- and bidentate phosphine ligands (such as PMe_2Ph or dppe).[24−26] Despite the extensive work on the characterization and catalytic application of cationic nonclassical ruthenium hydride complexes, the mechanistic details of their role in complex hydrogenation reactions remains largely unexplored. Recently, Chaplin and Dyson proposed a mechanism for the hydrogenation of alkenes using a Ru/TriPhos complex comprising nonclassical hydrides,[27] and Frediani and co-workers used a deuterium labeling study to provide first mechanistic insights for the hydrogenation of esters and lactones.[16]

Received: April 14, 2011
Published: July 25, 2011

Scheme 1. Reaction Sequences for the Hydrogenation/Dehydration of Levulinic Acid (LA, Top) and Itaconic Acid (IA, Bottom), Leading to the Corresponding Lactones, Diols, and Cyclic Ethers

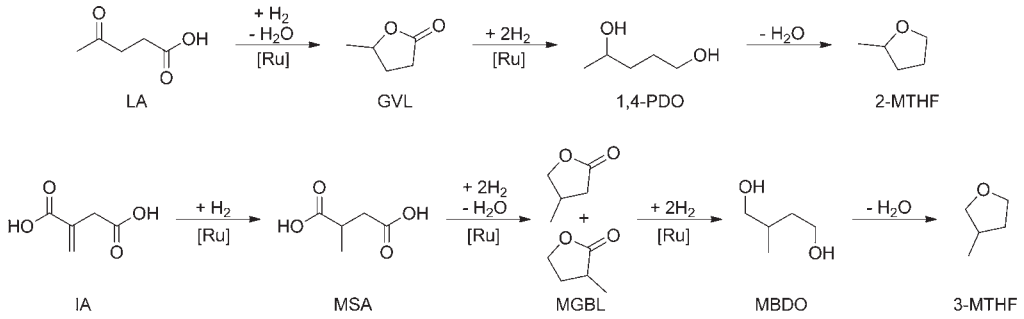

Chart 1. Catalyst System for the Hydrogenation of LA

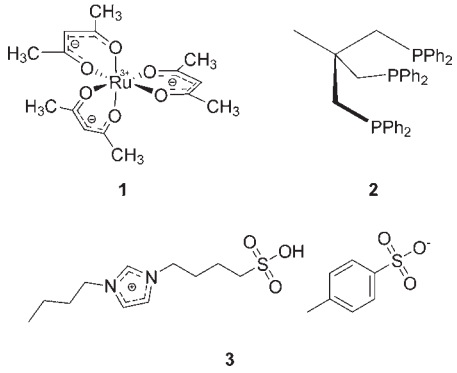

RESULTS

Experimental Background. During our work on levulinic acid reduction we were able to identify a well-defined organometallic species at the end of the hydrogenation reactions which could be isolated from experiments with higher catalyst loadings and finally characterized as [(TriPhos)Ru(CO)(H)$_2$] (**4**).[7] The formation of **4** can be explained by decarbonylation of trace amounts of aldehydes comprised in the reaction system. Aldehyde groups can be formed as intermediates during lactone reduction[7] or from dehydrogenation of the product alcohols, as was described by Cole-Hamilton for ethanol and by Hartwig for 1,4-butanediol in the presence of ruthenium−phosphine complexes.[28,29] The mechanistic aspects of these dehydrogenation reactions have been studied very recently computationally by Bühl and Bolm.[30,31] To verify the formation of **4** under hydrogenation conditions, the complex was synthesized independently using a modified reaction protocol. Thus, Ru(acac)$_3$ (**1**) and TriPhos (**2**) were dissolved in propanal and stirred for 20 h at 150 °C and 120 bar of hydrogen. Analytically pure **4** was isolated in 84% yield after precipitation with ethanol, making this also a synthetically useful procedure for **4** and related compounds. In addition to the liquid product propanol from catalytic hydrogenation, ethane could be identified in the gas phase, unequivocally demonstrating decarbonylation as the source of the CO ligand.

Using complex **4** as catalyst for hydrogenation of LA to γ-valerolactone (GVL), a slightly lower catalytic activity was observed as compared to the in situ system (Table 1, entries 1 and 4).

Table 1. Hydrogenation of LA and GVL with a Ruthenium TriPhos Catalyst[a]

				yield (%)		
entry	substrate	catalyst	additive	GVL	1,4-PDO[b]	2-MTHF[b]
1	LA	(**1** + **2**)[a]		3	95	0
2	GVL	(**1** + **2**)[a]		15	76	0
3	GVL	(**1** + **2**)[a]	**3**	1	0	95
4	LA	**4**[c]		22	73	3
5	GVL	**4**[c]		90	3	7
6	GVL	**4**[c]	**3**	1	0	96

[a] Conditions: 10 mmol of LA, 0.1 mol % Ru(acac)$_3$ (**1**), 0.2 mol % TriPhos (**2**), 1 mol % additive (**3**) where stated; reaction time, 18 h; hydrogen pressure $p(H_2)$ = 100 bar; 160 °C. [b] 1,4-PDO = 1,4-pentanediol, 2-MTHF = 2-methyltetrahydrofuran. [c] Conditions: 10 mmol LA, 0.1 mol % complex **4**, 1 mol % additive (**3**) where stated; reaction time, 18 h; hydrogen pressure $p(H_2)$ = 100 bar; 160 °C.

This was even more pronounced in the hydrogenation of GVL, where the isolated complex **4** proved almost inactive in accord with literature reports,[32] as compared to 85% conversion with the in situ catalyst (Table 1, entries 2 and 5). When an acidic additive such as the ionic liquid **3** (Chart 1) was present, the in situ catalyst and complex **4** showed similar activities toward the hydrogenation of GVL (Table 1, entries 3 and 6). Although the effect of the acidic additive on the rate of hydrogenation of GVL might be associated with acid catalyzed ring-opening of the lactone to form a more active substrate (vide infra), the increased rate for levulinic acid in the presence of acid suggests that complex **4** represents a resting state which is converted into the active species by protonation from LA and/or the acidic additive.[33] Indeed monitoring the reaction of complex **4** with LA under carefully controlled conditions by ^{1}H NMR at room temperature showed the clean formation of a monohydride species (Scheme 2, Figure 1), which could be characterized as complex **5** on the basis of mass spectroscopy (ESI, m/z = 841.6, 100%) and heteronuclear NMR spectroscopy.[34] The signal for the hydride is a doublet of doublets of doublets at −5.89 ppm and shows the characteristic $^3J_{PH}$ coupling with three different phosphorus atoms with a trans-coupling of 94.7 Hz and cis-couplings of 19.7 and 14.3 Hz, respectively. Taken together, these results strongly suggest that the complex fragment [(TriPhos)RuH]$^+$ defines the catalytically active center for the hydrogenation steps of the sequences shown in Scheme 1.[35]

dx.doi.org/10.1021/ja2034377 |J. Am. Chem. Soc. 2011, 133, 14349–14358

Scheme 2. Reaction of the Isolated Complex 4 with Levulinic Acid

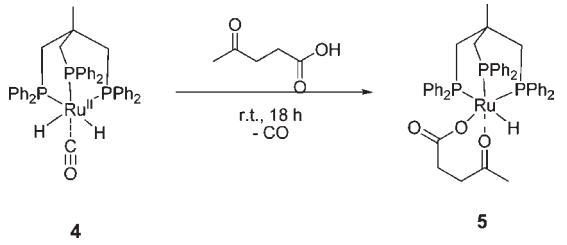

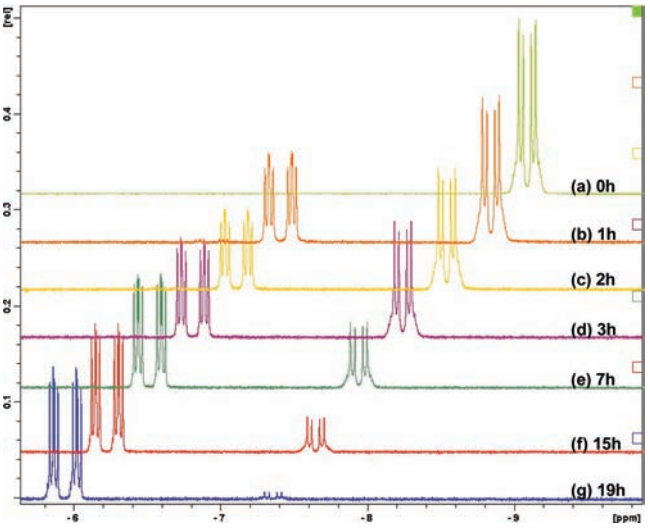

Figure 1. ^{1}H NMR spectra of the formation of **5** (g; $\delta = -5.89$ (ddd, 1H, $^3J_{P_{ax}-H} = 94.7$ Hz, $^3J_{P_{eq}-H} = 19.7$ Hz, $^3J_{P_{eq}-H}$ 14.3 Hz) ppm) from complex **4** (a; $\delta = -7.30$ (dd, 2H, $^3J_{P-H} = 50.2$ Hz, 18.3 Hz) ppm) in the presence of LA. Spectra measured after $t = 0$ (a), 1 (b), 2 (c), 3 (d), 7 (e), 15 (f), 19 h (g).

The formation of cationic Ru complexes starting from neutral ruthenium−dihydride complexes in the presence of TsOH or NH_4PF_6 under hydrogenation conditions was reported previously.[33,36] A dynamic equilibrium between the neutral dihydride *trans*-$[(dppm)_2Ru(H)_2]$ and the cationic hydrido−dihydrogen complex $[(dppm)_2HRu(H_2)]^+(OR)^-$ in the presence of hexafluoroisopropyl alcohol was observed by NMR spectroscopy.[37] Furthermore, the group of Elsevier reported very slow hydrogenation under neutral conditions, whereas the addition of HBF_4 increased both the rate of the first step and the selectivity toward the diol in the reduction of dimethylphthalate with the ruthenium−triphos system.[14] Comparable effects of acid were obtained in the present study for the hydrogenation of levulinic acid with the ruthenium−triphos system. After 5 h at 160 °C and 100 bar hydrogen, 52% GVL, 43% pentanediol (PDO), and 1% methyltetrahydrofuran MTHF were obtained in the absence of additives, whereas the addition of aIL and NH_4PF_6 as additives resulted in 91% MTHF and only 2% GVL. Product inhibition in pathways based on neutral ruthenium hydrides may be at least partly responsible for these differences.[38,39]

It is thus evident from the experimental data of the present study and related literature reports that the deep hydrogenation beyond the ester level is greatly facilitated under acidic conditions. This correlates with the fact that such conditions favor cationic intermediates, although acid catalyzed ring-opening of GVL could give a more active substrate than GVL itself and remains an alternative possibility. The clear positive effects of acid prompted us to chose the Triphos−ruthenium−hydride fragment in its cationic form $[(Triphos)RuH]^+$ as the common active species under the optimized reaction conditions and to investigate whether a unifying mechanism for all individual transformations in this catalytic system can be identified on the basis of this principle. We note, however, that this does not rule out the possibility of a neutral cycle where the first reduction steps would occur on neutral complexes such as **5**. Indeed, the direct hydride transfer in **5** to the coordinated carbonyl group has a low-lying transition state with an activation barrier of 7.3 kcal/mol. Further studies on the following steps and in particular on the activation energy for acid hydrogenation via the neutral cycle are currently under way.

Hydrogenation of Levulinic Acid, Step 1: Conversion to γ-Valerolactone (Scheme 3, Figure 2). Starting from the $[(Triphos)RuH]^+$ cation fragment, the structure **LA-1** provides a plausible entry into the catalytic cycle under strongly acidic conditions and high hydrogen pressure. The hydrogenation of LA is then initiated with the reduction of the keto group in **LA-1** to give the hydroxy acid which cyclizes to GVL (Scheme 3). The reduction is achieved by transfer of the classical hydride ligand to the carbon atom of the coordinated carbonyl group via a typical migratory insertion transition state **LA-TS 1−2** (Chart 2). The activation energy of this step amounts to 16.1 kcal/mol, while the product **LA-2** of the reaction is less stable than the reactants by 15.9 kcal/mol. The weak agostic interaction of the newly formed C−H bond in **LA-2** rearranges to a more stable conformation in which both oxygen atoms of the substrate coordinate to the metal center (**LA-3**).

In the next step, one hydrogen from the dihydrogen ligand is transferred as proton to the metal alkoxide group, while the other forms a bond to the metal center renewing the ruthenium hydride group (**LA-4**). The activation energy for this step is very low (4.8 kcal/mol, **LA-TS 3−4**, Chart 2) reflecting the efficient proton transfer in a four-membered transition state typical for σ-bond metathesis. In contrast to oxidative addition/reductive elimination, this pathway avoids the change of formal oxidation states and major rearrangements in the coordination sphere as also pointed out for example for the hydrogenolysis of rhodium−carboxylate groups.[40] The energetic span[41] for the overall reduction as defined by the TOF-determining-intermediate (TDI) **LA-1**, and the TOF-determining transition state (TDTS) **LA-TS 3−4** amounts to 17.1 kcal/mol, indicating the reaction to be possible under the given experimental conditions.

Replacing the γ-hydroxypentanoic acid from the catalyst by unreacted levulinic acid enables its lactonization to γ-valerolactone via well-known standard acid catalyzed organic mechanisms, which were not calculated in this study. Alternatively, cyclization could occur directly from **LA-4**, leading also back to **LA-1** in the presence of LA and H_2. Both pathways offer plausible routes for closing the catalytic cycle for this first hydrogenation.

Hydrogenation of LA, Step 2: Conversion of γ-Valerolactone to 1,4-Pentanediol under Acidic Conditions (Scheme 4, Figure 3). The next step in the hydrogenation sequence is the reduction of the lactone GVL. The ruthenium catalyzed hydrogenation of ester groups to the corresponding alcohols is of great synthetic value adding additional generic interest in this step.[42,43]

Scheme 3. Calculated Catalytic Cycle for the Hydrogenation of Levulinic Acid to γ-Valerolactone, Using the Cationic Complex LA-1 as the Catalyst (Phosphine Ligand Omitted for Clarity)

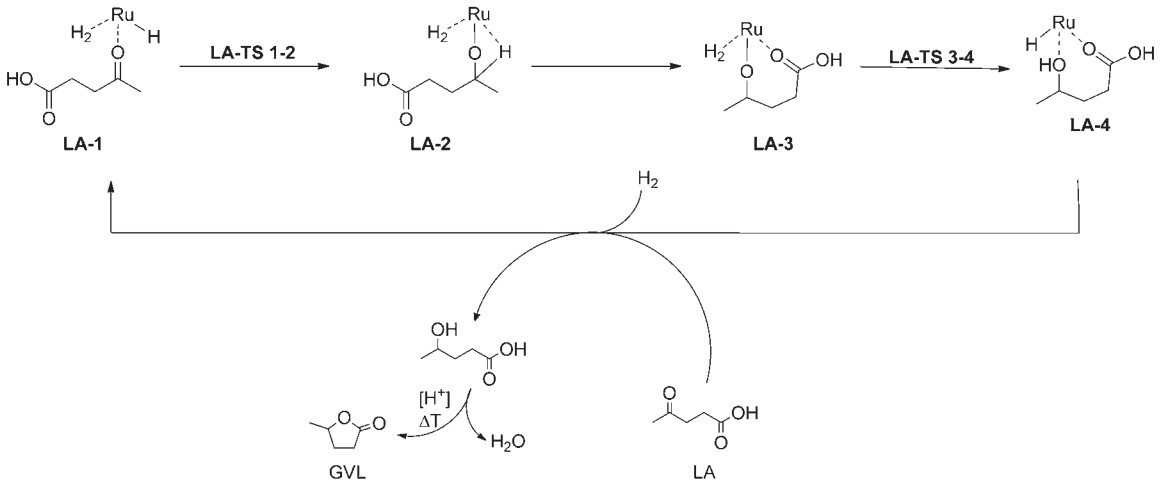

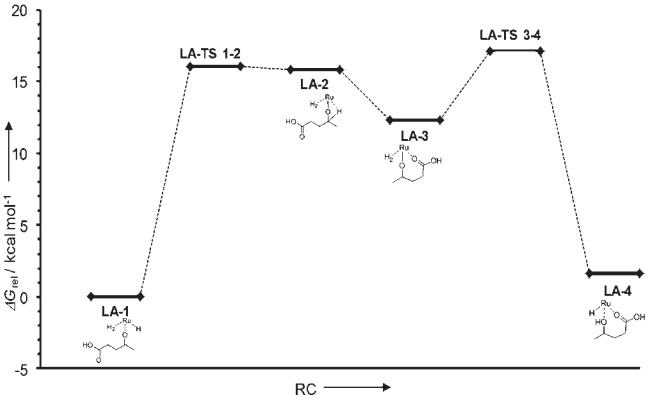

Figure 2. Energy profile for the hydrogenation of levulinic acid using **LA-1** as starting structure (Δ*G* in kilocalories per mole, relative to **LA-1**).

In analogy to LA, the primary hydrogenation product GVL can coordinate to the $[(TriPhos)RuH]^+$ fragment via its carbonyl group, leading to the starting complex **GVL-1** under H_2 pressure. The coordination via the carbonyl oxygen is the most prominent binding mode for esters and lactones in literature.[44−46] Only very few examples for coordination via the alkoxide or as a π-ligand are known.[47,48] In accord with this, geometry optimizations aiming at the localization of ether oxygen coordinated GVL did not result in stable structures for **GVL-1**. Again, a migratory insertion-type pathway for hydride transfer via transition state **GVL-TS 1−2** was found, leading to the lactolate complex **GVL-2**. Similar structures have been identified by NMR spectroscopy as intermediates for lactone hydrogenation by the group of Bergens.[39] The energy barrier for **GVL-TS 1−2** was determined to be 21.6 kcal/mol, which is significantly higher than for the corresponding step of the keto group hydrogenation in LA (16.1 kcal/mol). This is fully in line with the excellent selectivities that can be experimentally achieved in the consecutive reactions under optimized conditions. Even under identical conditions (160 °C, 100 bar) hydrogenation of LA to GVL is quantitative within 2 h whereas GVL conversion takes ca. 18 h with the in situ catalyst.

Proton transfer from the dihydrogen ligand to the ruthenium alkoxide leads to **GVL-3** with an activation energy of 14.7 kcal/mol. Again the four-membered transition state **GVL-TS 2−3** provides a pathway for the hydrogenolysis of the Ru−O bond that is lower in energy than the hydride transfer step. To proceed with the hydrogenation sequence, the coordinated lactole (cyclic hemiacetale) has to convert to its open hydroxy aldehyde form. Various pathways for this rearrangement within the coordination sphere of the ruthenium were investigated (paths I−III). Although transition states could be located in all cases, the energy barriers were found to be significantly higher than for the hydride transfer (path I, 25.8 kcal/mol; path II, 30.7 kcal/mol; path III, 26.7 kcal/mol). The energetic span for path I defined by **GVL-1** (TDI) and **GVL TS 3−5** (TDTS) amounts to 41.5 kcal/mol, and similar unrealistically high values result for paths II and III. Therefore, these routes can be ruled out to account for the further transformation.

In contrast, typical activation energies for the acid catalyzed opening of lactols are in the range of only 5 kcal/mol.[49,50] Thus, ring-opening of the free hemiacetal and recoordination of the hydroxyl aldehyde to give **GVL-6** provides a much lower energy pathway and is considered here as a productive route in the catalytic process. This assumption explains nicely the surprising experimental observation that hydrogenation of pure GVL to 1,4-PDO is significantly slower under acid-free conditions than the two-step conversion of LA (Table 1, entries 1 and 2). Application of the acidic additive **3** in the hydrogenation of GVL results in comparably high conversion as observed in the LA conversion (Table 1, entry 3). This can be rationalized if the barriers of paths I−III become rate limiting for pure GVL, whereas the ring opening is facilitated by H^+ from LA or the ionic liquid **3** and water from the condensation step in the case of consecutive reaction.

The final steps of the hydrogenation leading to the conversion of the hydroxy aldehyde in **GVL-6** to the diol in **GVL-9** are essentially identical to the previously discussed C═O hydrogenation sequences. The corresponding energy barriers are fairly low with activation energies of 9.0 kcal/mol for **GVL-TS 6−7** and 3.7 kcal/mol for **GVL-TS 8−9**. Ligand replacement of

Chart 2. Calculated Transition States of the LA Hydrogenation, LA-TS 1-2 Showing the Hydride Transfer to the Carbonyl Carbon and LA-TS 3-4 Showing the σ-Bond Metathesis for the Protonation of the Ru−O Bond

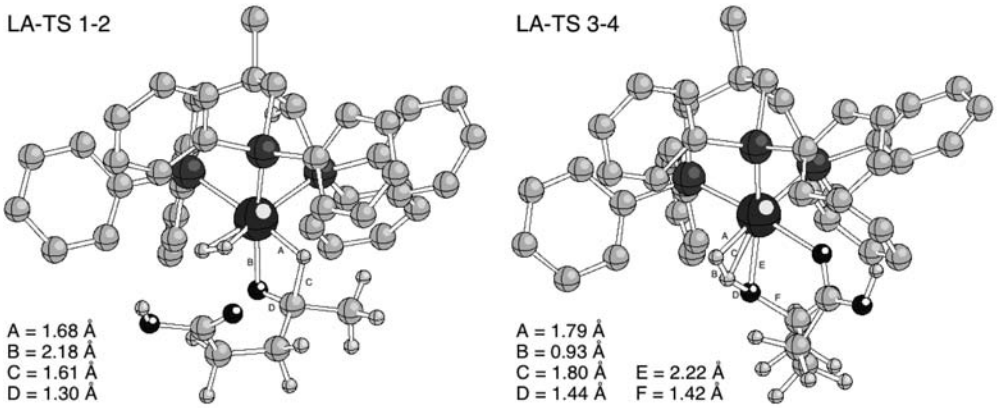

Scheme 4. Calculated Catalytic Cycle for the Hydrogenation of γ-Valerolactone to 1,4-Pentanediol under Acidic Conditions, Using the Monocationic GVL-1 as the Catalyst[a]

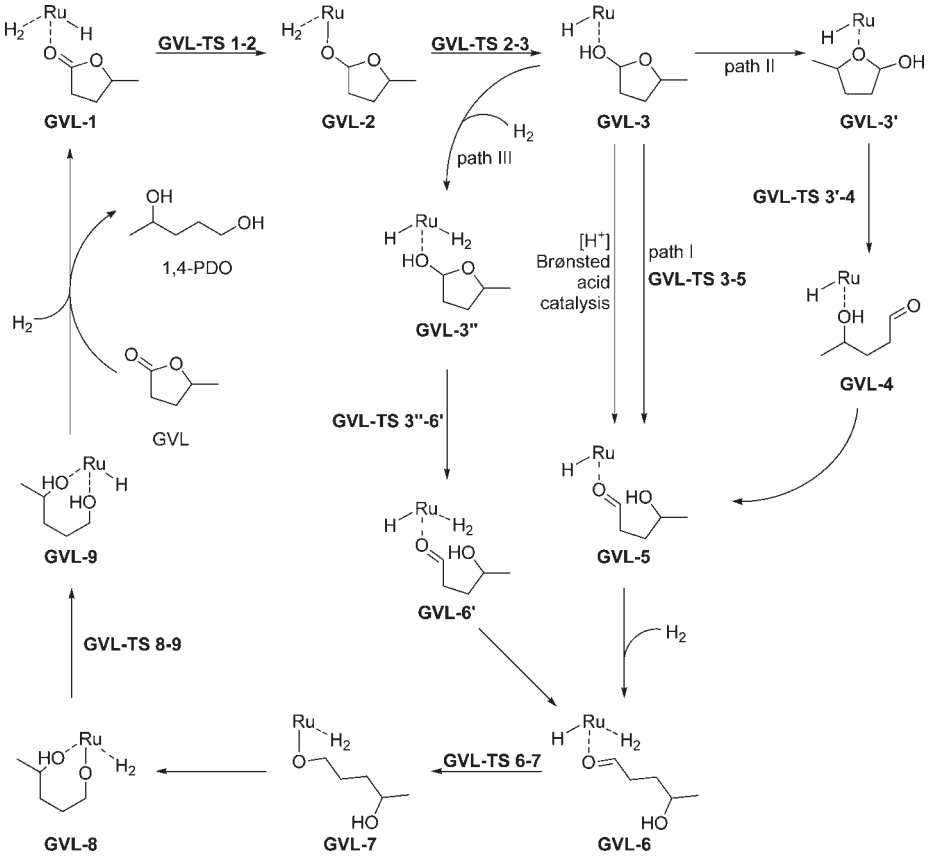

[a] The Brønstedt acid catalyzed pathway from **GVL-3** to **GVL-5** was not calculated. The phosphine ligand was omitted for clarity.

1,4-PDO by GVL closes the metal catalyzed cycle. Depending on the reaction conditions, the diol can undergo intramolecular etherification to 2-MTHF via well-established acid catalysis.

Hydrogenation of Itaconic Acid: Conversion of Methyl-succinic Acid to Methyl-γ-butyrolactone (Scheme 5, Figure 4). The Ru/TriPhos catalytic systems was shown to allow not only the hydrogenation of LA but also the conversion of IA to the corresponding lactones, diol, and cyclic ether in excellent yields (Scheme 1).[7] This transformation involves the catalytic hydrogenation of a free carboxylic acid function as a first step, a process that has very little precedent with homogeneous catalysts.[7,16] We therefore investigated whether the same basic mechanism at the $[(\text{TriPhos})\text{RuH}]^+$ fragment could be operative for free carboxylic acid groups.

Since the mechanistic aspects of hydrogenation of C−C double bonds with ruthenium phosphine complexes are

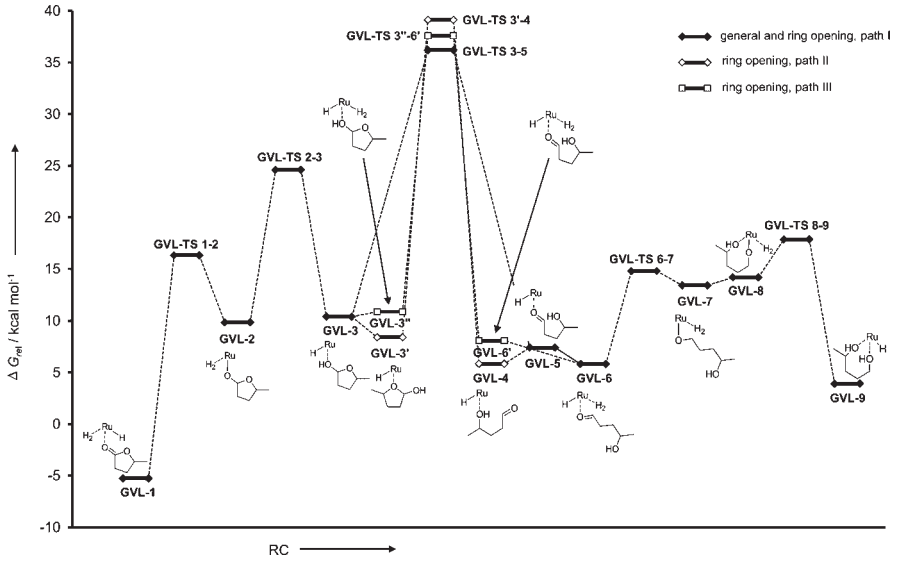

Figure 3. Energy profile for the hydrogenation of γ-valerolactone to 1,4-pentanediol using GVL-1 as the starting structure in structural analogy to **LA-1** (ΔG in kilocalories per mole, relative to **LA-1**).

Scheme 5. Calculated Catalytic Cycle for the Hydrogenation of Itaconic Acid to Methyl-γ-butyrolactone Using the Monocationic Complex IA-1 as the Catalyst (the Phosphine Ligand and the Charges of the Ru(II) Species Omitted for Clarity)

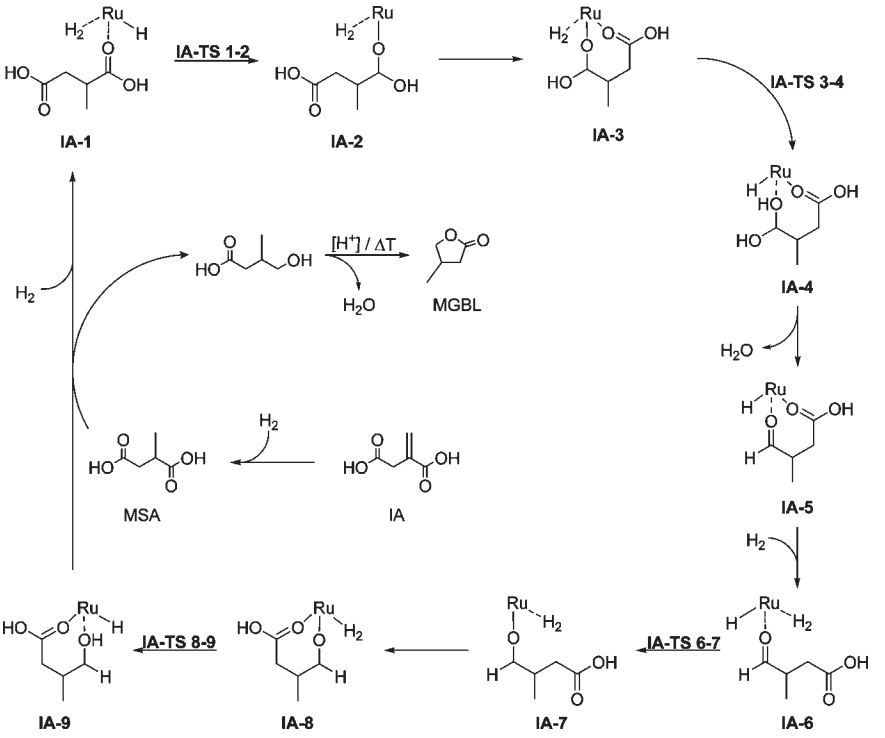

well-established,[51] the mechanistic cycle was started with methylsuccinic acid (MSA) as the primary hydrogenation product of IA. In analogy to the substrates discussed above, the complex **IA-1** could be located as a stable species on the energy surface and was used as a starting point.[52] The hydride transfer to the carboxylic carbon center occurs via transition state **IA-TS 1**−**2** (Chart 3), which is essentially identical to the pathway for the carbonyl reduction in LA. The activation energy to reach **IA-2** amounts to 24.2 kcal/mol and is thus 8.1 kcal/mol more demanding than the ketone reduction in LA (16.1 kcal/mol). This is fully in line with the experimental conditions that require significantly higher reaction temperatures for IA than for LA in the conversion to the corresponding lactones.[7]

The free coordination site at Ru in **IA-2** is readily occupied by the second carboxylic acid group to give **IA-3**, for which the proton transfer to the ruthenium alkoxide requires only an activation barrier of 8.1 kcal/mol via the σ-bond metathesis transition state **IA-TS 3**−**4**. Dehydration of the resulting geminal

dx.doi.org/10.1021/ja2034377 |J. Am. Chem. Soc. 2011, 133, 14349–14358

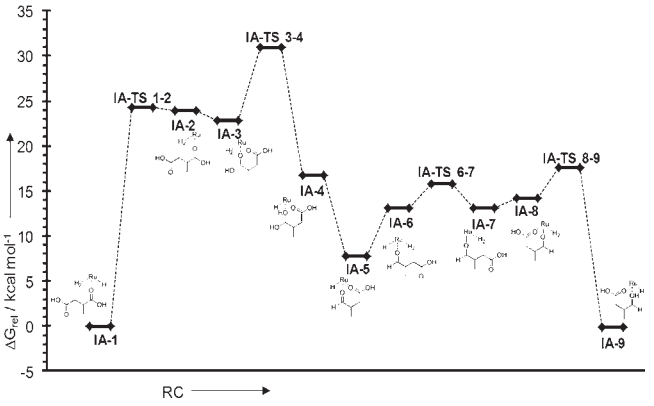

Figure 4. Energy profile for the hydrogenation of methylsuccinic acid to methyl-γ-butyrolactone using **IA-1** as the starting structure in analogy to **LA-1** (ΔG in kilocalories per mole, relative to **IA-1**).

Chart 3. Calculated Transition State IA-TS 1-2, Showing the Hydride Transfer to the Carboxyl Carbon

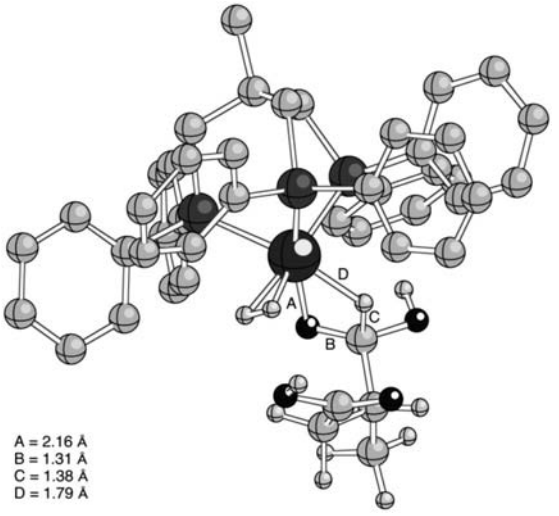

diol generates the significantly more stable aldehyde complex **IA-5**. The subsequent reduction of the aldehyde function follows again the established sequence with activation energies which are lower than the ones described above for the reduction of the aldehyde **GVL-6** ($\Delta G^{\ddagger}$ = 2.7 kcal/mol for **IA-TS 6**−**7** and 3.4 kcal/mol for **IA-TS 8**−**9**). The energetic spans reflect these findings as well: Complex **IA-1** and transition state **IA-TS 3**−**4** are the TDI and the TDTS, respectively, and define an energetic span of 31.0 kcal/mol for the carboxylic acid reduction, as compared to 17.1 kcal/mol for the reduction of the keto group in LA and only 7.0 kcal/mol for the reduction of the aldehyde in **GVL-6**.

Once methyl-γ-butyrolactone (MGBL) is formed, its further transformations can occur in full analogy to the isomeric GVL substrate. The calculated activation energies for the initial hydrogen transfer in MGBL hydrogenation are 19.8 kcal/mol (MGBL-TS 1−2, migratory insertion) and 18.3 kcal/mol (MGBL-TS 2−3, σ-bond metathesis) resulting in a total energetic span of 29.7 kcal/mol to be overcome by the system during this first lactone hydrogenation. This is in the same range as the energetic span of the free carboxylic acid reduction (31.0 kcal/mol). The high selectivity for MGBL at lower reaction temperatures results from substrate inhibition, based on greatly preferred coordination of the diacid over the corresponding lactone. This interpretation is supported by the concentration/time profiles of the consecutive hydrogenation steps, which show, an onset of the lactone reduction only after full conversion of the diacid.

CONCLUSION

Ruthenium phosphine catalysts and in particular the ruthenium/TriPhos system show a very promising potential for highly selective hydrogenation/dehydration pathways in the conversion of biogenic platform chemicals. Analyzing in detail a representative amount of individual steps of the resulting complex reaction networks, the present study shows that this can be associated with the ability to reduce the C═O functionality in aldehyde, ketone, ester, and even free carboxylic acid groups. These transformations can all be accomplished with a common mechanistic principle in the case of $[(\text{TriPhos})\text{RuH}]^+$ as the active center (Figure 5). Although a cycle involving neutral intermediates cannot be ruled out at this stage, the cationic cycle successfully explains the experimental activity trends.

In the common mechanistic scheme investigated here, the reduction results from a hydride transfer on to the carbonyl or carboxyl carbon via transition states typical for migratory insertion. The subsequent hydrogenolysis of the metal-oxide unit involves proton transfer via σ-bond metathesis from a coordinated dihydrogen molecule, regenerating at the same time the catalytically active Ru−H unit. The interplay between the classical and the nonclassical metal hydride coordination provides an overall pathway that does not require changes in the formal oxidation state of the ruthenium center.[40]

The heterolytic cleavage of the H_2 molecule and the associated proton transfer may be assisted by external basic centers of substrates or solvents potentially reducing the energy barrier for the hydrogenolysis steps even further.[53] This possibility was not yet assessed in the present study, because, in all mechanistic cycles investigated, the migratory insertion-type hydride transfer could be associated with the most energy demanding step. The activation barriers were found to range from 3 to 9 kcal/mol for the aldehydes (X = H) over 16 kcal/mol for the ketones (X = R) to 22−24 kcal/mol for the lactones (X = OR) and acids (X = OH), respectively. The energetic span,[41] which ultimately determines the catalytic turnover frequency for the overall reduction of the functional groups, increases in the same order. These results are fully in line with the observed experimental findings and allow rationalization of the optimized conditions for the selective transformations. Therefore, these mechanistic insights may provide guidelines also for future developments of efficient catalysts for challenging hydrogenation reactions of carboxylic acids and derivatives thereof.

COMPUTATIONAL DETAILS

All calculations in this work were performed with the Gaussian09 program series.[54] All structures were optimized using the dispersion corrected B97-D[55] functional together with the def2-SVP basis set for all elements and the associated ECP for ruthenium.[56−62] The automatic density fitting approximation was activated.[63,64] All structures were verified to be local minima or transition states by frequency calculation showing 0 and 1 imaginary frequencies, respectively. Free enthalpies and

Gibbs free energies reported include zero point energy corrections as well as thermal corrections for T = 298.15 K and p = 1 atm. For many structures IRC calculations were carried out additionally to prove the localized transition state connecting the expected local minima. For final evaluation of energies single-point calculations were carried out on the B97-D/def2-SVP geometries using the B97-D functional with def2-TZVP[56−62] basis set and associated ECP for ruthenium using the automatic density fitting approximation. Tables listing the energies obtained are included in the Supporting Information as well as Cartesian coordinates of all compounds. In the main text we refer to ΔG and $\Delta G^{\ddagger}$ values obtained using the def2-TZVP energies together with zero-point energy (zpe) corrections as well as thermal corrections from the lower level geometry optimizations unless noted otherwise. Table 2 summarizes relative energies ΔG_{rel} of all structures and activation barriers $\Delta G^{\ddagger}$ for all transition states (all in kilocalories per mole).

EXPERIMENTAL SECTION

Safety Warning. Experiments with compressed gases must be carried out only with appropriate equipment and under rigorous safety precautions.

General Comments. If not stated otherwise, handling of chemicals and manipulations were carried out under argon inert gas atmosphere using standard Schlenk techniques. $Ru(acac)_3$ was synthesized according to a procedure described by Knowles et al.[65] All chemicals were ordered from ABCR, Sigma-Alrich, or Fluka and used as received. Solvents were purified by distillation under argon atmosphere and subsequent storage over molecular sieves to remove traces of water.

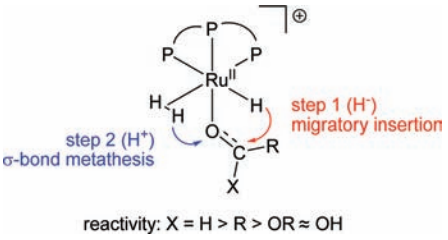

Figure 5. Schematic of production pathway.

Analytics. Conversion and selectivity of the catalytic reactions were determined via GC using a Thermo Focus or a Siemens Sichromat instrument, both equipped with flame ionizaiton detectors (FIDs). For the levulinic acid system a Cp-Sil-Pona-CB column was used with 1-hexanol as internal standard. Peaks were assigned via GC-MS and pure substance calibration. NMR spectra were recorded on a Bruker AV 400 spectrometer operating at 400.2 MHz for ^{1}H, and a Bruker AV 600 spectrometer operating at 600.1 MHz for ^{1}H. $CDCl_3$ or CD_2Cl_2 were used as the solvents. Chemical shifts of ^{1}H and ^{13}C NMR are reported relative to tetramethylsilane (TMS) with solvent residual protons and carbon atoms as internal standards, respectively. ^{31}P chemical shifts are reported relative to H_3PO_4.

Hydrogenation of LA to 1,4-Pentanediol. $Ru(acac)_3$ (3.9 mg, 10 μmol), 1,1,1-tris(diphenylphosphinomethyl)ethane (12.5 mg, 20.0 μmol), and levulinic acid (1.16 g, 10.0 mmol) and where applicable *N*-butyl-*N*′-(4-sulfobutyl)imidazolium *p*-toluenesulfonate (43.3 mg, 10.0 μmol) were placed in the glass liner of a 10 mL stainless steel reactor. The high-pressure reactor was repeatedly evacuated and flushed with argon and then pressurized with a predetermined amount of hydrogen to adjust a pressure of 100 bar after heating up to the appropriate reaction temperature. The mixture was stirred at the stated reaction temperature for the given time. After the reaction the vessel was cooled in an ice bath and slowly depressurized. The product mixture was analyzed by GC and ^{1}H NMR.

Hydrogenation of GVL to 1,4-Pentanediol. $Ru(acac)_3$ (3.9 mg, 10.0 μmol), 1,1,1-tris(diphenylphosphinomethyl)ethane (12.5 mg, 20.0 μmol), and where applicable *N*-butyl-*N*′-(4-sulfobutyl)-imidazolium *p*-toluenesulfonate (43.3 mg, 10.0 μmol) were placed in the glass liner of a 10 mL stainless steel reactor. The high-pressure reactor was repeatedly evacuated and flushed with argon, then GVL (1,05 g, 10.0 mmol) was added, and the reactor was pressurized with a predetermined amount of hydrogen to adjust to a pressure of 100 bar after heating to the appropriate reaction temperature. The mixture was stirred at the stated reaction temperature for the given time. After the reaction the

Table 2. Relative Energies ΔG_{rel} of All Structures and Activation Barriers $\Delta G^{\ddagger}$ for All Transition States (All in Kilocalories per Mole)

structure	ΔG	$\Delta G^{\ddagger}$	structure	ΔG	$\Delta G^{\ddagger}$	structure	ΔG	$\Delta G^{\ddagger}$
Scheme 3/Figure 2 [a]			GVL-6	5.8		Scheme 5/Figure 5 [b]		
LA-1	0.0		GVL-TS 6−7	14.8	9.0	IA-1	0.0	
LA-TS 1−2	16.1	16.1	GVL-7	13.4		IA-TS 1−2	24.2	24.2
LA-2	15.8		GVL-8	14.2		IA-2	23.9	
LA-3	12.3		GVL-TS 8−9	17.8	3.7	IA-3	22.8	
LA-TS 3−4	17.1	4.8	GVL-9	3.9		IA-TS 2−4	31.0	8.1
LA-4	1.6					IA-4	16.7	
			Scheme 4/Figure 3, path II [a]			IA-5	7.7	
Scheme 4/Figure 3, path I [a]			GVL-3′	8.4		IA-6	13.0	
GVL-1	−5.3		GVL-TS 3′-4	39.1	30.7	IA-TS 6−7	15.7	2.7
GVL-TS 1−2	16.3	21.6	GVL-4	5.8		IA-7	13.1	
GVL-2	9.9					IA-8	14.1	
GVL-TS 2−3	24.6	14.7	Scheme 4/Figure 3, path III [a]			IA-TS 8−9	17.6	3.4
GVL-3	10.4		GVL-3″	10.9		IA-9	−0.1	
GVL-TS 3−5	36.2	25.8	GVL-TS 3″-6′	37.6	26.7	MGBL-1	−2.7	
GVL-5	7.4		GVL-6′	8.1		MGBL-TS 1−2	17.2	19.8
						MGBL-2	8.7	
						MGBL-TS 2−3	27.0	18.3

[a] Relative to LA-1. [b] Relative to IA-1.

dx.doi.org/10.1021/ja2034377 |J. Am. Chem. Soc. 2011, 133, 14349–14358

vessel was cooled in an ice bath and slowly depressurized. The product mixture was analyzed by GC and ^{1}H NMR.

Hydrogenation of LA or GVL with Complex 4 as the Catalyst. Where applicable, *N*-butyl-*N*′-(4-sulfobutyl)imidazolium *p*-toluenesulfonate (4.3 mg, 5.0 μmol) was placed in the glass liner of a 10 mL stainless steel reactor. The high-pressure reactor was repeatedly evacuated and flushed with argon; then complex **4** (3.9 mg, 5.0 μmol) dissolved in degassed LA (0.51 g, 5.0 mmol) or GVL (0.5 g, 5.0 mmol) was transferred via syringe. The reactor was pressurized with a predetermined amount of hydrogen to adjust a pressure of 100 bar after heating to the appropriate reaction temperature. The mixture was stirred at the stated reaction temperature for the given time. After the reaction the vessel was cooled in an ice bath and slowly depressurized. The product mixture was analyzed by GC.

Synthesis of Carbonyldihydrido(1,1,1-tris(diphenylphosphinomethyl)ethane)ruthenium(II) (4). A glass liner of a 10 mL stainless steel high-pressure reactor was loaded with $Ru(acac)_3$ (**1**; 100 mg, 0.25 mmol, 1 equiv) and TriPhos (**2**; 174.9 mg, 0.27 mmol, 1.1 equiv) and the liner was equipped with a magnetic stirrer bar and transferred into the corresponding reactor. The atmosphere was changed to argon, and propanal (2.5 mL) was added. The reactor was pressurized with 120 bar of hydrogen and stirred for 20 h at 150 °C. The reactor was cooled to 0 °C, and the pressure was released into a rubber balloon. The product mixture was transferred into a Schlenk flask and ethanol (1 mL) was added. The solution was filtered off, and the solid was washed with ethanol (1 mL) twice to yield the product (**4**) as light yellow powder (166.3 mg, 0.21 mmol, 84%). $RuC_{15}H_{21}O$ MW: 785.14 g/mol. ^{1}H NMR (600 MHz, CD_2Cl_2, 25 °C): δ 7.68 (t, 8 H, $^3J_{HH}$ = 7.8 Hz, arom), 7.32 (t, 4 H, $^3J_{HH}$ = 8.7 Hz, arom), 7.17 (t, 2 H, $^3J_{HH}$ = 7.2 Hz, arom), 7.06−7.14 (m, 8 H, H-12, arom), 7.02 (m, 8 H, arom), 2.31 (dd, 2 H, $^3J_{PH}$ = 15.1 Hz, $^2J_{HH}$ = 6.5 Hz, CH_2 equatorial), 2.20 (dd, 2 H, $^3J_{PH}$ = 15.1 Hz, $^2J_{HH}$ = 6.5 Hz, CH_2 equatorial), 2.13 (d, 2 H, $^3J_{PH}$ = 8.2 Hz, CH_2 axial), 1.52 (s, 3 H, CH_3), −7.30 ppm. (dd, 2 H, $^3J_{PH}$ = 18.3 Hz, 50.2 Hz, Ru−H). ^{31}P NMR (242.9 MHz, CD_2Cl_2, 25 °C): δ 34.5 (t, 1 P, $^3J_{PP}$ = 31.2 Hz, P-axial), 26.7 ppm (d, 2 P, $^3J_{PP}$ = 31.2 Hz, P-equatorial). ^{13}C NMR (150.1 MHz, CD_2Cl_2, 25 °C): δ 209.5, 139.8, 138.0, 132.4, 131.1, 128.6, 128.4, 127.8, 127.5, 38.8, 38.4, 35.0, 33.5 ppm.

Reaction of Carbonyldihydrido(1,1,1-tris-(diphenylphosphinomethyl)ethane)ruthenium(II) (4) with Levulinic Acid. In an NMR tube complex **4** (15.5 mg, 21 μmol) was dissolved in CD_2Cl_2 (0.7 mL). Levulinic acid (4.0 mg, 34 μmol) was added, and the mixture was shaken for 30 s. The color of the solution changed from light yellow to orange within the first 10 min. After 15 min the first ^{1}H NMR was recorded and for the next 18 h ^{1}H NMR were recorded hourly. *m*/*z*: 841.6 (calc: 842.2). ^{1}H NMR (600 MHz, CD_2Cl_2, 25 °C): δ 7.96 (m, 2 H, arom), 7.80 (m, 2 H, arom) 7.56 (m, 2 H, arom), 7.32 (m, 1 H, arom), 7.36 (m, 2 H, arom), 7.25 (m, 2 H, arom), 7.08 (m, 1 H, arom), 6.99 (m, 1 H, arom), 6.78 (m, 2 H, arom), 2.72 (m, 2 H, LA-CH_2), 2.62 (m, 2 H, LA-CH_2), 2.48 (m, 1 H, TriPhos-CH_2), 2.46 (m, 1 H, TriPhos-CH_2), 2.38 (m, 1 H, TriPhos-CH_2), 2.37 (m, 1 H, TriPhos-CH_2), 2.29 (m, 1 H, TriPhos-CH_2), 2.25 (s, 3 H, LA-CH_3), 2.23 (m, 1 H, TriPhos-CH_2), 2.16 (m, 1 H, TriPhos-CH_2), 1.59 (m, 3 H, TriPhos-CH_3), −5.89 ppm (ddd, 1 H, $^3J_{P_{ax}H}$ = 94.7 Hz, $^3J_{P_{eq}H}$ = 19.7 Hz, $^3J_{P_{eq}H}$ = 14.3 Hz, Ru−H). ^{31}P NMR (242.9 MHz, CD_2Cl_2, 25 °C): δ 47.8 (dd, 1 P, $^3J_{PP}$ = 40.2 Hz, $^3J_{PP}$ = 19.0 Hz, P-equatorial), 19.0 (dd, 1 P, $^3J_{PP}$ = 40.2 Hz, $^3J_{PP}$ = 28.9 Hz, P-equatorial), 4.4 ppm (dd, 1 P, $^3J_{PP}$ = 28.9 Hz, $^3J_{PP}$ = 19.0 Hz, P-axial).

■ ASSOCIATED CONTENT

Supporting Information. Tables listing all calculated energies in hartrees and Cartesian coordinates for all structures and the text giving the complete ref 54. This material is available free of charge via the Internet at http://pubs.acs.org.

■ AUTHOR INFORMATION

Corresponding Author

leitner@itmc.rwth-aachen.de; klankermayer@itmc.rwth-aachen.de

■ ACKNOWLEDGMENT

This work was supported by the Cluster of Excellence "Tailor Made Fuels from Biomass" (TMFB), which is funded by the Excellence Initiative of the German federal and state governments to promote science and research at German universities. We are grateful for generous allocation of computer time by the Centre for Computing and Communication (RZ) of RWTH Aachen University. We thank Mrs. Ines Bachmann-Remy for the acquisition of the 600 MHz NMR spectra.

■ REFERENCES

(1) Ragauskas, A. J.; Williams, C. K.; Davison, B. H.; Britovsek, G.; Cairney, J.; Eckert, C. A.; Frederick, W. J., Jr.; Hallett, J. P.; Leak, D. J.; Liotta, C. L.; Mielenz, J. R.; Murphy, R.; Templer, R.; Tschaplinski, T. *Science* **2006**, *311*, 484.

(2) Kamm, B.; Kamm, M.; Gruber, P. R.; Kromus, S. In *Biorefineries—Industrial Processes and Products. Status Quo and Future Directions*; Kamm, B., Gruber, P. R., Kamm, M., Eds.; Wiley-VCH: Weinheim, Germany, 2006; Vol. 1, p 3.

(3) Corma, A.; Iborra, S.; Velty, A. *Chem. Rev.* **2007**, *107*, 2411.

(4) Huber, G. W.; Iborra, S.; Corma, A. *Chem. Rev.* **2006**, *106*, 4044.

(5) *Top Value-Added Chemicals from Biomass — Results of Screening for Potential Candidates from Sugars and Synthesis Gas*; Werpy, T.; Petersen, G., Eds.; U.S. Department of Energy: Washington, DC, 2004, Vol. 1.

(6) Bozell, J. J.; Petersen, G. R. *Green Chem.* **2010**, *12*, 539.

(7) Geilen, F. M. A.; Engendahl, B.; Harwardt, A.; Marquardt, W.; Klankermayer, J.; Leitner, W. *Angew. Chem., Int. Ed.* **2010**, *49*, 5510.

(8) Van Engelen, M. C.; Teunissen, H. T.; de Vries, J. G.; Elsevier, C. J. *J. Mol. Catal. A: Chem.* **2003**, *206*, 185.

(9) Comprehensive Asymmetric Catalysis, Jacobsen, E. N.; Pfaltz, A.; Yamamoto, H., Eds. Springer, Heidelberg, Germany, 1999.

(10) Hara, Y.; Wada, K. *Chem. Lett.* **1991**, 553.

(11) Mehdi, H.; Fábos, V.; Tuba, R.; Bodor, A.; Mika, L. T.; Horváth, I. T. *Top. Catal.* **2008**, *48*, 49.

(12) Ohkuma, T.; Noyori, R. In *Handbook of Homogeneous Hydrogenation*; de Vries, J. G., Elsevier, C. J., Eds.; Wiley-VCH: Weinheim, Germany, 2007; Vol. 4, p 1105.

(13) Teunissen, H. T.; Elsevier, C. J. *Chem. Commun.* **1997**, 667.

(14) Teunissen, H. T.; Elsevier, C. J. *Chem. Commun.* **1998**, 1367.

(15) Nunez, A. A.; Eastham, G. R.; Cole-Hamilton, D. J. *Chem. Commun.* **2007**, 3154.

(16) Rosi, L.; Frediani, M.; Frediani, P. *J. Organomet. Chem.* **2010**, *695*, 1314.

(17) Bianchini, C.; Meli, A.; Moneti, S.; Vizza, F. *Organometallics* **1998**, *17*, 2636.

(18) Bianchini, C.; Meli, A.; Moneti, S.; Oberhauser, W.; Vizza, F.; Herrera, V.; Fuentes, A.; Sanchez-Delgado, R. A. *J. Am. Chem. Soc.* **1999**, *121*, 7071.

(19) Bianchini, C.; Meli, A.; Peruzzini, M.; Vizza, F.; Zanobini, F. *Coord. Chem. Rev.* **1992**, *120*, 193.

(20) Belkova, N. V.; Bakhmutova, E. V.; Shubina, E. S.; Bianchini, C.; Peruzzini, M.; Bakhmutov, V. I.; Epstein, L. M. *Eur. J. Inorg. Chem.* **2000**, 2163.

(21) Bianchini, C.; Moneti, S.; Peruzzini, M.; Vizza, F. *Inorg. Chem.* **1997**, *36*, 5818.

(22) Bakhmutov, V. I.; Bianchini, C.; Peruzzini, M.; Vizza, F.; Vorontsov, E. V. *Inorg. Chem.* **2000**, *39*, 1655.

(23) Bakhmutov, V. I.; Bakhmutova, E. V.; Belkova, N. V.; Bianchini, C.; Epstein, L. M.; Masi, D.; Peruzzini, M.; Shubina, E. S.; Vorontsov, E. V.; Zanobini, F. *Can. J. Chem.* **2001**, *75*, 479.
(24) Lough, A. J.; Morris, R. H.; Ricciuto, L.; Schleis, T. *Inorg. Chim. Acta* **1998**, *270*, 238.
(25) Albinati, A.; Klooster, W. T.; Koetzle, T. F.; Fortin, J. B.; Ricci, J. S.; Eckert, J.; Fong, T. P.; Lough, A. J.; Morris, R. H.; Golombek, A. P. *Inorg. Chim. Acta* **1997**, *259*, 351.
(26) Grocott, S. C.; Skelton, B. W.; White, A. H. *Aust. J. Chem.* **1983**, *36*, 259.
(27) Chaplin, A. B.; Dyson, P. J. *Inorg. Chem.* **2008**, *47*, 381.
(28) Morton, D.; Cole-Hamilton, D. J.; Utuk, I. D.; Paneque-Sosa, M.; Lopez-Poveda, M. *J. Chem. Soc., Dalton Trans.* **1989**, 489.
(29) Zhao, J.; Hartwig, J. F. *Organometallics* **2005**, *24*, 2441.
(30) Sieffert, N.; Bühl, M. *J. Am. Chem. Soc.* **2010**, *132*, 8056.
(31) Johansson, A. J.; Zuidema, E.; Bolm, C. *Chem.—Eur. J.* **2010**, *16*, 13487.
(32) (a) Kilner, M.; Tyers, D. V.; Crabtree, S. P.; Wood, M. A. Davy Process Technology Ltd., London, U.S. Patent Application 2005/0234269 A1, 2005. (b) Wood, M.; Crabtree, S. P.; Tyers, D. V.; WO05/051875, 2005.
(33) Hara, Y.; Kusaka, H.; Inagaki, H.; Takahashi, K.; Wada, K. *J. Catal.* **2000**, *194*, 188.
(34) When the acidic ionic liquid **3** was used as a proton source, formation of a similar monohydridic fragment was observed. Compared to levulinic acid, the reaction was fast at room temperature and gas formation was observed.
(35) The possibility of one PPh_2 group of TriPhos temporarily opening up an additional coordination site has been demonstrated by Horváth in rhodium-catalyzed hydroformylation: Kiss, G.; Horváth, I. T. *Organometallics* **1991**, *10*, 3798 This may provide additional pathways for example on the basis of $[(P\cap P2)Ru(CO)H]^+$ or $[(P\cap P2)RuH]^+$ fragments. All transformations in the present study could be accomplished on the basis of three coordination sites in facial proximity.
(36) Rappert, T.; Yamamoto, A. *Organometallics* **1994**, *13*, 4984.
(37) Ayllon, J. A.; Gervaux, C.; Sabo-Etienne, S.; Chaudret, B. *Organometallics* **1997**, *16*, 2000.
(38) Zhao, J.; Hartwig, J. F. *Organometallics* **2005**, *24*, 2441.
(39) Takebayashi, S.; Bergens, S. H. *Organometallics* **2009**, *28*, 2349.
(40) (a) Hutschka, F.; Dedieu, A.; Leitner, W. *Angew. Chem., Int. Ed. Engl.* **1995**, *34*, 1742. (b) Hutschka, F.; Dedieu, A.; Eichberger, M.; Fornika, R.; Leitner, W. *J. Am. Chem. Soc.* **1997**, *119*, 4432.
(41) (a) Kozuch, S.; Shaik, S. *J. Am. Chem. Soc.* **2006**, *128*, 3355. (b) Uhe, A.; Kozuch, S.; Shaik, S. *J. Comput. Chem.* **2011**, *32*, 978. (c) Kozuch, S.; Shaik, S. *Acc. Chem. Res.* **2011**, *44*, 101.
(42) Saudan, L. A.; Saudan, C. M.; Debieux, C.; Wyss, P. *Angew. Chem., Int. Ed.* **2007**, *46*, 7473.
(43) (a) Zhang, J.; Leitus, G.; Ben-David, Y.; Milstein, D. *Angew. Chem., Int. Ed.* **2006**, *45*, 1113. (b) Zhang, J.; Leitus, G.; Ben-David, Y.; Milstein, D. *J. Am. Chem. Soc.* **2009**, *127*, 12429.
(44) Shambayati, S.; Crowe, W. E.; Schreiber, S. L. *Angew. Chem., Int. Ed. Engl.* **1990**, *29*, 256.
(45) Evans, D. A.; Rovis, T.; Kozlowski, M. C.; Tedrow, J. S. *J. Am. Chem. Soc.* **1999**, *121*, 1994.
(46) Daley, C. J. A.; Bergens, S. H. *J. Am. Chem. Soc.* **2002**, *124*, 3680.
(47) Kapoor, P.; Pathak, A.; Kapoor, R.; Venugopalan, P.; Corbella, M.; Rodríguez, M.; Robles, J.; Llobet, A. *Inorg. Chem.* **2002**, *41*, 6153.
(48) Meiere, S. H.; Ding, F.; Friedman, L. A.; Sabat, M.; Harman, W. D. *J. Am. Chem. Soc.* **2002**, *124*, 13506.
(49) Meng, Q.; Zhang, C.; Huang, M.-B. *Can. J. Chem.* **2009**, *87*, 1610.
(50) Lebedev, A.; Leite, L.; Fleisher, M.; Stonkus, V. *Chem. Heterocycl. Compd.* **2000**, *36*, 775.
(51) *Handbook of Homogeneous Hydrogenation*; de Vries, J. G., Elsevier, C. J., Eds.; Wiley-VCH: Weinheim, Germany, 2007.
(52) The sodium carboxylates of MSA and IA could not be hydrogenated with the present catalytic system. This experimental finding is in line with the free acid rather than the carboxylate group as starting point. The cycle was studied for only one of the two very similar carboxylic acid functions, as only marginal differentiation of the two regioisomers is observed experimentally.[7]
(53) Dobereiner, G. E.; Nova, A.; Schley, N. D.; Hazari, N.; Miller, S. J.; Eisenstein, O.; Crabtree, R. *J. Am. Chem. Soc.* **2011**, *133*, 7547.
(54) Frisch, M. J. et al. *Gaussian 09*, Revision A.02; Gaussian: Wallingford, CT, 2009.
(55) Grimme, S. *J. Comput. Chem.* **2006**, *27*, 1211.
(56) Weigend, F.; Ahlrichs, R. *Phys. Chem. Chem. Phys.* **2005**, *7*, 3297.
(57) Schaefer, A.; Horn, H.; Ahlrichs, R. *J. Chem. Phys.* **1992**, *97*, 2571.
(58) Schaefer, A.; Huber, C.; Ahlrichs, R. *J. Chem. Phys.* **1994**, *100*, 5829.
(59) Eichkorn, K.; Weigend, F.; Treutler, O.; Ahlrichs, R. *Theor. Chem. Acc.* **1997**, *97*, 119.
(60) Weigend, F.; Furche, F.; Ahlrichs, R. *J. Chem. Phys.* **2003**, *119*, 12753.
(61) Andrae, D.; Haeussermann, U.; Dolg, M.; Stoll, H.; Preuss, H. *Theor. Chim. Acta* **1990**, *77*, 123.
(62) Metz, B.; Stoll, H.; Dolg, M. *J. Chem. Phys.* **2000**, *113*, 2563.
(63) Dunlap, B. I. *J. Chem. Phys.* **1983**, *78*, 3140.
(64) Dunlap, B. I. *J. Mol. Struct. (THEOCHEM)* **2000**, *529*, 37.
(65) Knowles, T. S.; Howells, M. E.; Howlin, B. J.; Smith, G. W.; Amodio, C. A. *Polyhedron* **1994**, *13*, 2197.